

# Robust Field Map Estimation Using Both Global and Local Minima

H. Kim<sup>1,2</sup>, K. Sung<sup>1</sup>, and B. A. Hargreaves<sup>1</sup>

<sup>1</sup>Department of Radiology, Stanford University, Stanford, CA, United States, <sup>2</sup>Electrical Engineering, Stanford University, Stanford, CA, United States

**Introduction:** A variety of field-map estimation techniques using 3-pt multi-echo acquisitions have been developed for reliable water-fat separation [1-6]. The field-map is mainly estimated by finding a minimum of a cost function, defined as  $\|S - \hat{S}\|_2^2$ , the difference between measured data and estimated data with field-map values varying, which is periodic with period  $(1/\Delta TE)$ . However, there still exists an ambiguity in water or fat-dominant area since a cost function in that region has multiple minima whose amplitudes are too similar to reliably identify the true global minimum as shown in Fig.1. To address this ambiguity problem, this study proposes a robust field-map estimation method using both global and local minima. The main contributions of this study lie in demonstrating that there are at most two minima during a period in a cost function, and suggesting three steps to determine an initial seed pixel to make a region growing process more secure.

**Methods:** In this work, a cost function is efficiently generated by L1-norm of Discrete Fourier Transform (DFT) of three echoes, proposed in [6]. To save the computations, all operations are processed at 1/4 or 1/8 fold down-sampled data. Foreground mask is produced by cropping the region whose intensity is larger than 10 percent of all pixels' magnitudes.

As illustrated in Fig.2, two factors, water-fat phase difference and the proportion of water, affect the number of minima in a cost function during a period at each pixel. This demonstrates that the number of minima can be one in certain conditions, while it does not exceed two, which implies that one of the two minima should be the true solution. Thus, the local minimum can offer a true solution where the global minimum does not consistently correspond to a genuine field-map. Based on this observation, the first step is to find two minima at each pixel.

Secondly, a region growing process is applied for smoothness of field-map. It is essential to accurately determine an initial seed with a true field-map for successful region growing. For that objective, this work suggests: **A)** As stated in [4], pixels with single minimum inside foreground are believed to have a genuine field-map value, so it tries to find those locations. But pixels with single minimum are confined under strict conditions, as seen in Fig.2. **B)** Alternative is to find pixels whose ratio of local minimum to global maximum in cost function is greater than about 0.3. In water or fat region, that ratio is quite low, as shown in Fig. 1. Thus, it is the way to avoid setting an initial seed at water or fat area where field-map estimation is unreliable. **C)** The final stage is to search a center of region having low standard deviations of global minima, empirically less than 50 with 3x3 matrix size. Mostly, however, an initial seed was successfully determined before the last stage. Defining pixels satisfying a condition as super pixels, an initial seed is chosen considering both median of global minima in those pixels and distance to center of mass, as stated in [3]. Region growing is simply performed by choosing one of the two minima that are closer to the previously determined field-map with an assumption of smoothness.

Finally, for accuracy checking that is required to correct the failure in region growing, an 8x8 matrix divides the field-map image at the coarsest level, measuring standard deviation and mean of field-map values inside foreground in each block, extract blocks with standard deviation over 50, and taking a region growing process again with reference to the mean of the spatially closest block with standard deviation below 50. This process repeats with smaller block size, 4x4 and 2x2, for more delicate correction. Finally, two-fold bilinear interpolation gets the image bigger, and accuracy checking is implemented in finer level as well. With resulting field-map, water-fat separation is achieved by least-squares operation.

Abdominal and knee imaging were acquired using a 1.5T GE scanner with IDEAL SPGR with 8 channel multi-coil: TE= [1.98,3.57,5.16] ms, TR= 10ms, and BW= 83.3kHz.

**Results:** To validate the performance, the proposed method was compared with a technique suggested in [4]. It shows more consistent performance in water-fat separation, especially in edge region for both cases, as shown in Fig.3. It can be thought that proposed method serves more secure way to determine an initial seed having a genuine field-map, which results in more precise field-map estimation and water-fat separation.

**Discussion:** We demonstrate that a robust field-map can be achieved by using two minima and more secure way of determining an initial seed. This is based on the result of the simulation, varying the proportion of water and water-fat phase difference, which the number of minima in a cost function ranges from one to two. Also, a reliable method of determining an initial seed enables the region growing process to more successfully perform field-map estimation. With multi-frequency of fat spectrum modeling combined, more accurate fat information can be obtained.

**Conclusion** The proposed method using both minima and setting a reliable initial seed offers an effective approach to robust field-map estimation.

## References

- [1] Glover et al, MRM 1991;18:371-383
- [2] Reeder et al, MRM 2005;54:636-644
- [3] Yu et al, MRM 2005;54:1032-1039
- [4] Lu et al, MRM 2008;60:236-244
- [5] Hernando et al, MRM 2008;59:571-580
- [6] Tsao et al, ISMRM 2008;16:653

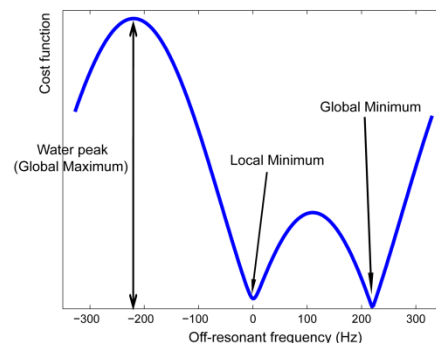


**Fig. 1** Cost function in a pixel inside water region in 1.5T IDEAL-SPGR phantom data.

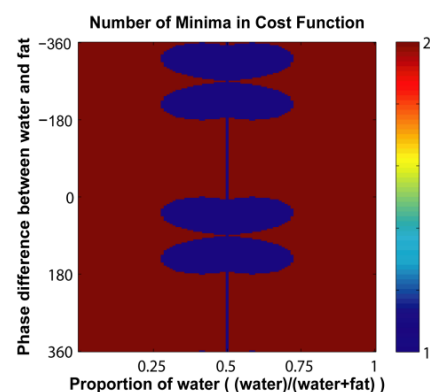


**Fig. 2** The number of minima in a cost function during a period, which is a result of the simulation, varying the proportion of water and water-fat phase difference

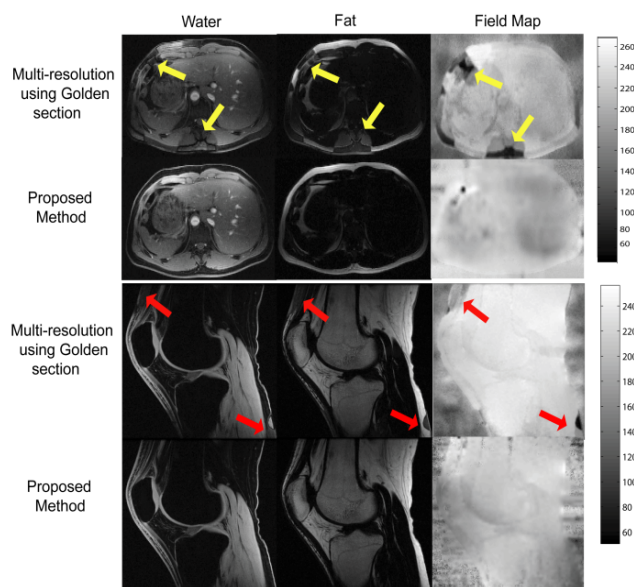


**Fig. 3** Water, fat and field-map images from abdominal and knee imaging at 1.5T IDEAL-SPGR. Arrows indicate failure of water-fat separation. Proposed method showed stable performance in both cases.